Bis(alkynyl) Mercury(II) Complexes of Oligothiophenes and Bithiazoles

Wai-Yeung Wong,* Ka-Ho Choi, and Guo-Liang Lu

Department of Chemistry, Hong Kong Baptist University, Waterloo Road, Kowloon Tong, Hong Kong, People's Republic of China

Zhenyang Lin

Department of Chemistry, The Hong Kong University of Science and Technology, Clearwater Bay, Hong Kong, People's Republic of China

Received July 1, 2002

A new class of binuclear mercury(II) bis(alkynyl) complexes containing oligothiophenes and bithiazoles as the central organic linkers are reported. The d^{10} mercury(II) complexes [R′HgC≡CRC≡CHgR′] (R = thiophene-2,5-diyl, [2,2′]bithiophene-5,5′-diyl, [2,2′:5′,2″]terthiophene-5,5″-diyl, 4,4′-di(*tert*-butyl)-2,2′-bithiazole-5,5′-diyl, 4,4′-di(*p*-methoxyphenylene)-2,2′-bithiazole-5,5′-diyl; R′ = Me, Ph) were prepared in high yields by the dehydrohalogenation reaction of the appropriate mercury(II) chloride precursors with the diethynyl-functionalized oligothiophenes and bithiazoles under basic medium. Structural elucidation of these compounds was made by FTIR and NMR spectroscopies and FAB mass spectrometry. The solid-state molecular structures of [MeHgC≡CRC≡CHgMe] (R = thiophene-2,5-diyl, [2,2′]-bithiophene-5,5′-diyl) established by X-ray crystallography reveal that a loose polymeric structure is formed in each case through weak intermolecular noncovalent Hg···Hg interactions. All the complexes have been demonstrated to exhibit rich absorption and luminescence behavior as a function of the number of thiophene rings as well as the electronic nature of the five-membered rings within the bridging ligand. With increasing thiophene content, the absorption and emission features are both red-shifted and the emission quantum yields are increased. In the presence of electron-withdrawing imine nitrogen atoms, the optical spectra for the bithiazole derivatives also show a significant bathochromic shift as compared to their bithienyl counterparts.

Introduction

There is a continuing interest in the design of alkynylgold(I) complexes owing to the potential applications of these compounds in many areas of materials science and crystal engineering.[1] Studies of weak intermolecular d^{10}−d^{10} Au···Au bonding interactions in gold(I) systems and how these can influence conformations, crystal packing, and chemical transformations represent a challenging area of research.[1,2] The rich photochemistry associated with this class of luminescent gold(I) complexes has also aroused much attention in the development of optoelectronic devices.[1,2] Several recent reports have shown that alkynylgold(I) complexes containing phosphine or isocyanide ligands exhibit strong emission spectra.[1] In contrast to the body of work on discrete and polymeric alkynylgold(I) species, related studies on the isoelectronic mercury(II) system remain relatively unexplored, presumably due to the poor solubility of oligomeric organomercurial substances. To the best of our knowledge, studies of linear binuclear alkynylmercury(II) complexes are very rare.[3] On the basis of the isolobal analogy between $[Au(PPh_3)]^+$ and $[HgR]^+$ (R = Me, Ph) fragments,[4] we envisioned that a comparative investigation of the alkynylmercury(II) complexes to their gold(I) congeners will be a valuable addition to this important area of research.

Within the family of species that are involved in the biogeochemical cycle of mercury, organomercurials, especially methyl- and arylmercury compounds, are the major and the most deleterious mercury contaminant

* To whom correspondence should be addressed. E-mail: rwywong@hkbu.edu.hk. Fax: (852)3411-7348.

(1) (a) Puddephatt, R. J. *Coord. Chem. Rev.* **2001**, *216−217*, 313, and references therein. (b) Puddephatt, R. J. *Chem. Commun.* **1998**, 1055. (c) Yam, V. W.-W.; Chan, C.-L.; Li, C.-K.; Wong, K. M.-C. *Coord. Chem. Rev.* **2001**, *216−217*, 173, and references therein. (d) Yam, V. W.-W.; Li, C.-K.; Chan, C.-L. *Angew. Chem., Int. Ed.* **1998**, *37*, 2857. (e) Yam, V. W.-W.; Lo, K. K.-W. *Chem. Soc. Rev.* **1999**, *28*, 323. (f) Müller, T. E.; Choi, S. W.-K.; Mingos, D. M. P.; Murphy, D.; Williams, D. J.; Yam, V. W.-W. *J. Organomet. Chem.* **1994**, *484*, 209. (g) Irwin, M. J.; Vittal J. J.; Puddephatt, R. J. *Organometallics* **1997**, *16*, 3541. (h) Hunks, W. J.; MacDonald, M.-A.; Jennings, M. C.; Puddephatt, R. J. *Organometallics* **2000**, *19*, 5063. (i) Tzeng, B.-C.; Lo, W.-C.; Che, C.-M.; Peng, S.-M. *J. Chem. Soc., Chem. Commun.* **1996**, 181. (j) Whittall, I. R.; Humphrey, M. G.; Houbrechts, S.; Persoons, A. *Organometallics* **1996**, *15*, 5738.

(2) (a) Sladek, A.; Schmidbaur, H. *Inorg. Chem.* **1996**, *35*, 3268. (b) Mingos, D. M. P.; Yau, J.; Menzer S.; Williams, D. J. *Angew. Chem., Int. Ed. Engl.* **1995**, *34*, 1894. (c) Schmidbaur, H.; Dziwok, K.; Grohmann, A.; Muller, G. *Chem. Ber.* **1989**, *122*, 893. (d) Li, D.; Hong, X.; Che, C.-M.; Lo, W.-C.; Peng, S.-M. *J. Chem. Soc., Dalton Trans.* **1993**, 2929.

(3) Wong, W.-Y.; Choi, K.-H.; Lu, G.-L.; Shi, J.-X.; Lai, P.-Y.; Chan, S.-M.; Lin, Z. *Organometallics* **2001**, *20*, 5446.

(4) (a) Hoffmann, R. *Angew. Chem., Int. Ed. Engl.* **1982**, *21*, 711. (b) Miessler, G. L.; Tarr, D. A. *Inorganic Chemistry*; Prentice Hall: New Jersey, 1999; Chapter 15.

10.1021/om020517e CCC: $22.00
Publication on Web 09/11/2002

agents that can be detected.[3,5] Considerable efforts are currently devoted to the search for the rapid and sensitive separation and detection procedures for these species.[6,7] To address this problematic issue, various approaches have been employed, and derivatization procedures that convert Hg(II) and MeHg(II) species into organometallic acetylides (e.g., $(PhC{\equiv}C)_2Hg$ and PhC≡CHgMe) for chromatographic analysis have been demonstrated to be effective measures with regards to this goal.[7] Recent studies have shown that acetylides carrying the dansyl and acridone frameworks are promising luminescent labels for MeHg(II).[8] Following our recent reports of the synthesis and optical spectroscopy of some platinum and ferrocenyl acetylide compounds with oligothienyl bridges,[9] it seemed an attractive goal to us to expand this system to the d^{10} mercury complexes. Our interest in metal acetylide polymers and their molecular precursors incorporating oligothienyl moieties stems from the fact that π-conjugation of organometallic units into the oligothiophene chain offers intriguing models that possess unique properties that are not accessible in the classical organic counterparts.[9,10] Here we describe the synthesis, characterization, and luminescence behavior of a series of bis(alkynyl) mercury(II) complexes with oligothiophene and bithiazole linking units (Chart 1). The crystal structures of [MeHgC≡CRC≡CHgMe] (R = thiophene-2,5-diyl, [2,2′]bithiophene-5,5′-diyl) have been established to study the metal−metal and ligand−ligand interactions in mercury polyyne systems.

Results and Discussion

Syntheses and Spectroscopic Properties. The ligand precursors **Ib**−**IIIb** were prepared by previously reported procedures.[9a] 4,4′-Di(*tert*-butyl)-2,2′-bithiazole

Chart 1

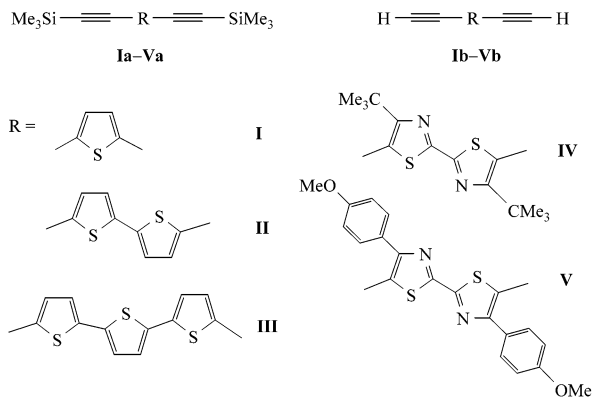

Scheme 1

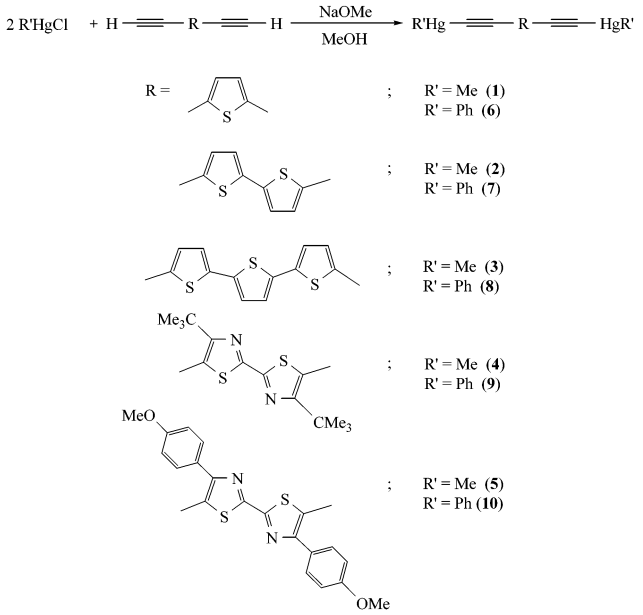

was synthesized in 74% yield by the reaction of 1-bromopinacolone and dithiooxamide in refluxing ethanol.[11,12] Starting with 2-bromo-4′-methoxyacetophenone, 4,4′-di(*p*-methoxyphenylene)-2,2′-bithiazole can similarly be made. Bromination of both species with Br_2 afforded the 5,5′-dibromo derivatives in moderate yields, which can then furnish the Me_3Si-protected compounds **IVa** and **Va** as yellow solids via the well-established palladium-catalyzed cross-coupling reaction with trimethylsilylacetylene.[9a,12,13] Upon deprotection with K_2CO_3 in MeOH, **IVa** and **Va** were converted into the terminal acetylene-functionalized bithiazoles **IVb** and **Vb**, respectively. Both **IVb** and **Vb** are stable in air at room temperature.

The reaction pathways leading to the new binuclear alkynylmercury(II) complexes are shown in Scheme 1. Following the classical dehydrohalogenating route, treatment of 2 equiv of MeHgCl or PhHgCl with each of the bifunctional diethynyl ligands **Ib**−**Vb** in an excess of

(5) (a) O'Neill, P. *Environmental Chemistry*; Chapman & Hall: London, 1993; Chapter 14. (b) Wang, Y. S.; Carty, A. J.; Chieh, C. *J. Chem. Soc., Dalton Trans*. **1977**, 1801. (c) Bach, R. D.; Weibel, A. T. *J. Am. Chem. Soc.* **1976**, *98*, 6241. (d) Rabenstein, D. L. *Acc. Chem. Res.* **1978**, *11*, 100. (e) Rabenstein, D. L.; Reid, R. S. *Inorg. Chem*. **1984**, *23*, 1246. (f) Arnold, A. P.; Carty, A. J.; Reid, R. S.; Rabenstein, D. L. *Can. J. Chem*. **1985**, *63*, 2430. (g) Moore, M. J.; Distefano, M. D.; Zydowsky, L. D.; Cummings, R. T.; Walsh, C. T. *Acc. Chem. Res*. **1990**, *23*, 301.

(6) (a) Puk, R.; Weber, J. H. *Appl. Organomet. Chem*. **1994**, *8*, 293. (b) Alcock, N. W.; Lampe, P. A.; Moore, P. *J. Chem. Soc., Dalton Trans*. **1980**, 1471. (c) Ghilardi, C. A.; Midollini, S.; Orlandini, A.; Vacca, A. *J. Chem. Soc., Dalton Trans*. **1993**, 3117. (d) Ghilardi, C. A.; Innocenti, P.; Midollini, S.; Orlandini, A.; Vacca, A. *J. Chem. Soc., Chem. Commun*. **1992**, 1691. (e) Baumann, T. F.; Reynolds, J. G.; Fox, G. A. *Chem. Commun*. **1998**, 1637. (f) Huang, S.-P.; Franz, K. J.; Arnold, E. H.; Devenyi, J.; Fish, R. H. *Polyhedron* **1996**, *15*, 4241.

(7) (a) Fabbri, D.; Lombardo, M.; Trombini, C.; Vassura, I. *Appl. Organomet. Chem*. **1995**, *9*, 713. (b) Fabbri, D.; Trombini, C. *Chromatographica* **1994**, *39*, 246. (c) Rapsomanikis, S. *Analyst* **1994**, *119*, 1429.

(8) Bolletta, F.; Fabbri, D.; Lombardo, M.; Prodi, L.; Trombini, C.; Zaccheroni, N. *Organometallics* **1996**, *15*, 2415.

(9) (a) Lewis, J.; Long, N. J.; Raithby, P. R.; Shields, G. P.; Wong, W.-Y.; Younus, M. *J. Chem. Soc., Dalton Trans*. **1997**, 4283. (b) Chawdhury, N.; Köhler, A.; Friend, R. H.; Wong, W.-Y.; Lewis, J.; Younus, M.; Raithby, P. R.; Corcoran, T. C.; Al-Mandhary, M. R. A.; Khan, M. S. *J. Chem. Phys*. **1999**, *110*, 4963. (c) Wong, W.-Y.; Lu, G.-L.; Ng, K.-F.; Choi, K.-H.; Lin, Z. *J. Chem. Soc., Dalton Trans*. **2001**, 3250.

(10) (a) Manners, I. *Angew. Chem., Int. Ed. Engl*. **1996**, *35*, 1602. (b) Kingsborough, R. P.; Swager, T. M. *Prog. Inorg. Chem*. **1999**, *48*, 123. (c) Pollagi, T. P.; Stoner, T. C.; Dallinger, R. F.; Gilbert, T. M.; Hopkins, M. D. *J. Am. Chem. Soc*. **1991**, *113*, 703. (d) Calabrese, J. C.; Cheng, L.-T.; Green, J. C.; Marder, S. R.; Tam, W. *J. Am. Chem. Soc*. **1991**, *113*, 7227. (e) Meyers, L. K.; Langhoff, C.; Thompson, M. E. *J. Am. Chem. Soc*. **1992**, *114*, 7560. (f) Lichtenberger, D. L.; Renshaw, S. K.; Bullock, R. M. *J. Am. Chem. Soc*. **1993**, *115*, 3276.

(11) (a) Nanos, J. I.; Kampf, J. W.; Curtis, M. D. *Chem. Mater*. **1995**, *7*, 2232. (b) Yamamoto, T.; Suganuma, H.; Maruyama, T.; Inoue, T.; Muramatsu, Y.; Arai, M.; Komarudin, D.; Ooba, N.; Tomaru, S.; Sasaki, S.; Kubota, K. *Chem. Mater*. **1997**, *9*, 1217.

(12) Wong, W.-Y.; Chan, S.-M.; Choi, K.-H.; Cheah, K.-W.; Chan, W.-K. *Macromol. Rapid Commun*. **2000**, *21*, 453.

(13) Takahasi, S.; Kuroyama, Y.; Sonogashira K.; Hagihara, N. *Synthesis* **1980**, 627.

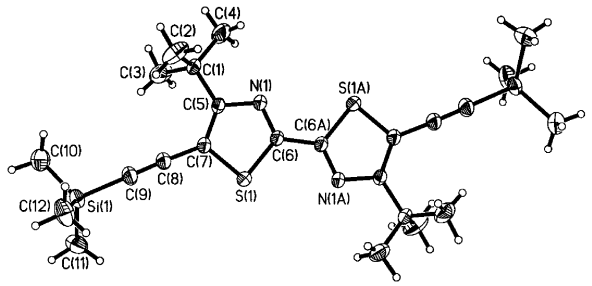

Figure 1. Molecular structure of **IVa** with 25% probability thermal ellipsoids.

NaOMe in MeOH readily provided the dimercury(II) diacetylide complexes [R′HgC≡CRC≡CHgR′] (R = thiophene-2,5-diyl, R′ = Me (**1**), Ph (**6**); [2,2′]bithiophene-5,5′-diyl, R′ = Me (**2**), Ph (**7**); [2,2′:5′,2″]terthiophene-5,5″-diyl, R′ = Me (**3**), Ph (**8**); 4,4′-di(*tert*-butyl)-2,2′-bithiazole-5,5′-diyl, R′ = Me (**4**), Ph (**9**); 4,4′-di(*p*-methoxyphenylene)-2,2′-bithiazole-5,5′-diyl, R′ = Me (**5**), Ph (**10**)) in very good yields.[3,7a,8] The reaction is complete after stirring at room temperature for 15 h, and the products can be precipitated from the solution mixture. All these new compounds were isolated as air-stable yellow to orange solids in high purity and exhibit fairly good solubility in chlorinated solvents such as CH_2Cl_2 and $CHCl_3$. They were satisfactorily characterized by spectroscopic (IR, ^{1}H NMR, and MS) and analytical methods.

All the spectroscopic data of compounds **1**−**10** are consistent with their structures (Experimental Section). The IR spectra of these complexes display a single characteristic ν(C≡C) absorption band in the range 2115−2130 cm^{-1} and confirm the linear arrangement in such Hg(II) systems. The ν(C≡C) values of the Hg(II) complexes are lower than those of the corresponding terminal or Me_3Si-substituted acetylide ligands.[14] The C≡C*H* stretching vibration in the reactants is absent in the product structure. The ^{1}H NMR spectra of **1**−**10** all show features pertaining to the protons of the heteroaromatic and other organic groups. In each case, we can detect the respective molecular ion peak $[M]^+$ or $[MH]^+$ in the FAB mass spectra.

Crystal Structure Analysis. The molecular structures of compounds **IVa** and **Va** are shown in Figures 1 and 2, respectively, and selected structural parameters are combined and given in Table 1. In each case, the molecule sits on a crystallographic center of symmetry at the midpoint of the C−C bond between the two nearly planar thiazole rings and the rings adopt a *trans* geometry on steric grounds. The mean sulfur−carbon length is 1.717(2) (**IVa**) and 1.727(3) Å (**Va**), which can be compared with those found in the platinum(II) acetylide derivative (1.729(9) Å) and the bithienyl precursor **IIa** (1.730(6) Å).[9a] The C−C triple bond is typical of other reported acetylide bonds. For **Va**, the thiazole and C_6H_4 planes are almost coplanar (dihedral angle 3.2°). However, no significant interheteroatom contacts or π-stacking interactions are observed in both cases.

The solid-state structures of complexes **1** and **2** are illustrated in Figures 3 and 4, respectively, and key

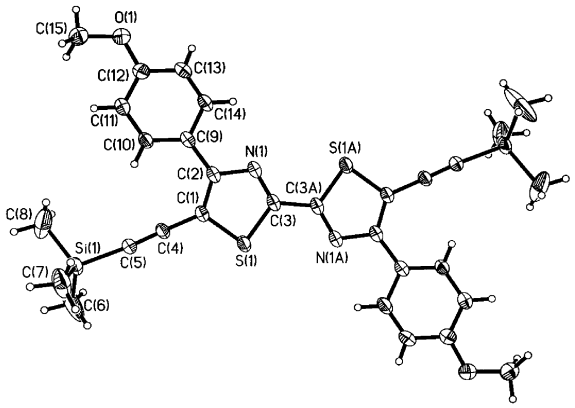

Figure 2. Molecular structure of **Va** with 25% probability thermal ellipsoids.

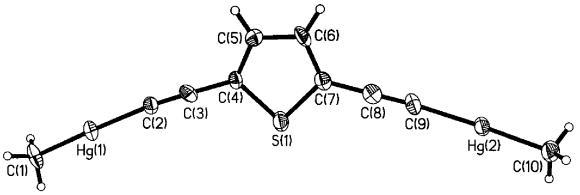

Figure 3. Molecular structure of **1** with 25% probability thermal ellipsoids.

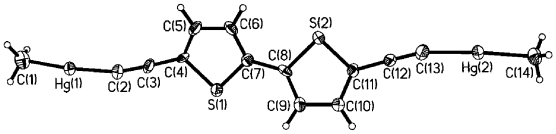

Figure 4. Molecular structure of **2** with 25% probability thermal ellipsoids.

Table 1. Selected Bond Lengths (Å) and Angles (deg) for Compounds IVa and Va

	IVa	Va
Si(1)−C(sp)	1.839(3)	1.839(3)
C(sp)−C(sp)	1.192(3)	1.203(4)
C(sp)−C(sp^2)	1.421(3)	1.424(3)
Si(1)−C(sp)−C(sp)	176.3(3)	175.2(3)
C(sp)−C(sp)−C(sp^2)	176.9(3)	178.8(3)

Table 2. Selected Bond Lengths (Å) and Angles (deg) for Compounds 1 and 2

	1	2
Hg(1)−C(sp^3)	2.065(13)	2.06(2)
Hg(2)−C(sp^3)	2.052(14)	2.07(2)
Hg(1)−C(sp)	2.036(13)	2.02(2)
Hg(2)−C(sp)	2.042(13)	2.05(2)
C(2)−C(3)	1.202(18)	1.26(3)
C(8)−C(9)	1.196(18)	
C(12)−C(13)		1.22(3)
C(sp^3)−Hg(1)−C(sp)	176.0(5)	174.3(10)
C(sp^3)−Hg(2)−C(sp)	177.8(6)	175.4(10)
Hg(1)−C(sp)−C(sp)	174.2(11)	166(2)
Hg(2)−C(sp)−C(sp)	175.4(14)	166(2)

bond lengths and angles are listed in Table 2. In each case, the crystal structure consists of discrete dimeric molecules in which the mercury centers adopt a two-coordinate linear geometry to afford the expected rodlike skeleton. Reminiscent of the PAuC≡C unit in the analogous gold(I) complexes, the isoelectronic MeHgC≡C fragment displays similar structural motifs in **1** and **2**. The Hg−C(alkyne) bonds are slightly longer than the Au−C(alkyne) bonds in the isostructural complexes Ph_3-

(14) Manna, J.; John, K. D.; Hopkins, M. D. *Adv. Organomet. Chem.* **1995**, *38*, 79.

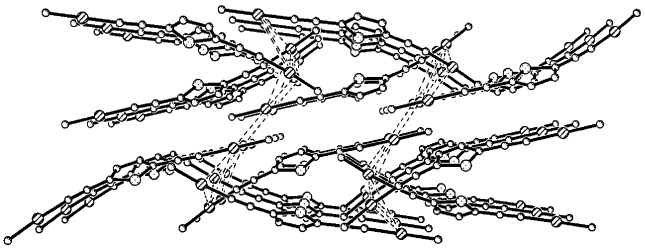

Figure 5. Crystal-packing diagram for **1** showing the weak Hg···Hg intermolecular contacts in a 3D network.

$PAuC{\equiv}CRC{\equiv}CAuPPh_3$ (R = thiophene-2,5-diyl, 1.997(6) and 2.005(6) Å; [2,2′]bithiophene-5,5′-diyl, 2.004(4) Å)[15] but comparable to those in other Hg(II) acetylide compounds.[3,16] The Hg−CH_3 bond (ca. 2.05(1)−2.07(2) Å) appears to be shorter than those found in some methylmercury(II) complexes with thiol ligands such as $[(MeHg)_2(S_2C_6H_{10})]$ (2.08(2)−2.12(2) Å)[6b] and $[MeC(CH_2SHgMe)_3]$ (2.09(3)−2.13(3) Å).[6c] The C≡C bond lengths in the ethynyl bridge are fairly typical of metal acetylide σ-bonding (1.196(18), 1.202(18) Å for **1**; 1.22(3), 1.26(3) Å for **2**). For **2**, the two thiophene rings exhibit *anti*-configuration to minimize the repulsion between the β-hydrogens on the adjacent rings. What is perhaps remarkable in both structures is the presence of weak intermolecular noncovalent Hg···Hg interactions (3.777, 3.935 Å for **1**, 3.851 Å for **2**), which links the molecular units together to form a loose polymeric structure. Although alkynylgold(I) complexes exhibiting Au···Au interactions are numerous,[1,2] literature reports concerning d^{10}−d^{10} Hg···Hg intermolecular contacts are, to our knowledge, very scarce. In a related study, the formation of polymeric gold acetylide systems through aurophilic Au···Au interactions is restricted to complexes with only one thienyl ring between the two acetylenic units in the digold oligothiophene systems.[15] For **1**, the lattice is stabilized through extensive Hg···Hg interactive vectors in a 3D arrangement (Figure 5), and the closest intermolecular nonbonded Hg···S contact is due to the Hg(2)···S(1) interaction (4.072 Å). There are also short contacts involving the thienyl sulfur and methyl hydrogen atoms (S(1)···H(1A) 2.999 Å, S(1)···H(10A) 2.952 Å). Intermolecular interactions between acetylenic C−C bonds and hydrogen atoms on the thiophene or methyl group are apparently located (C(2)···H(5A) 2.953 Å, C(3)···H(10C) 3.072 Å). An inspection of the crystal-packing diagram of **2** (Figure 6) accounts for the large dihedral angle (ca. 26.7°) between the two thiophene planes. The S(2)-ring twists to accommodate intermolecular, electrostatic S(2)···H(1A) (2.795 Å) and Hg(1)···H(9A) (3.248 Å) interactions in **2**. We also observe a short contact between Hg(1) and S(2) (3.752 Å) which probably arises from the donation of electron density from the lone pair on the sulfur atom to an empty hybrid orbital on the mercury. The lattice structure is highlighted by the presence of weak Hg···Hg interactions in a 2D network (Figure 6).

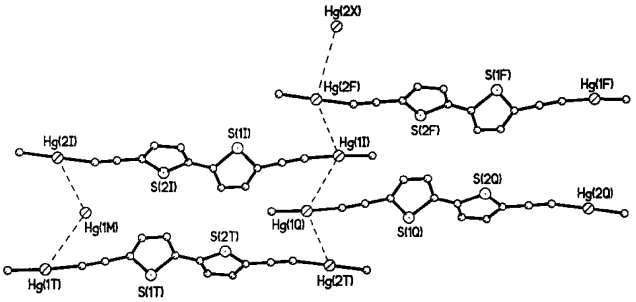

Figure 6. Crystal-packing diagram for **2** showing the weak Hg···Hg intermolecular contacts in a 2D network.

Table 3. Electronic Absorption and Emission Data for the Mercury(II) Complexes 1−10 and Their Organic Counterparts

compound	λ_{max}/nm ($\epsilon \times 10^{-4}$/M^{-1} cm^{-1})[a]	λ_{em}/nm (Φ)[a]
Ib	293 (0.06), 305sh (0.06)	359 (0.019)
IIb	344sh (0.2), 355 (2.2)	392sh, 411 (0.058)
IIIb	393 (2.4)	444, 467sh (0.086)
IVb	372 (2.5)	414sh, 431 (0.066)
Vb	290 (5.5), 399 (1.6)	465 (0.024)
1	318 (2.5), 337 (2.5)	361 (0.007)
2	348 (2.6), 368 (2.6), 384 (2.3)	409 (0.025)
3	412 (3.0)	461, 490sh (0.067)
4	393 (3.9), 414sh (2.5)	460, 488sh (0.050)
5	297 (4.8), 413 (2.5), 430sh (2.3)	470 (0.016)
6	323 (0.4), 341 (0.3)	361sh, 394 (0.006)
7	348 (2.4), 368 (2.8), 384 (2.4)	417sh, 439 (0.020)
8	412 (2.8)	464, 494sh (0.069)
9	393 (4.3), 414sh (0.3)	435, 458 (0.043)
10	299 (4.8), 414 (2.8), 438sh (0.2)	468 (0.014)

[a] In CH_2Cl_2. sh = shoulder.

Absorption and Luminescence Properties. The electronic absorption and emission data of new dimercury(II) diyne compounds **1**−**10** together with **Ib**−**Vb** in CH_2Cl_2 are given in Table 3. In general, the absorption spectra of the mercury(II) complexes display intense bands in the range 297−438 nm, and the peak maxima are shifted to longer wavelength as compared to those of the free alkynes. The strong dependence of the solution absorption spectra on the nature of the central linker unit suggests the absorption peaks to arise from ligand-localized π−π* transitions, and the apparent insensitivity of these bands toward the hydrocarbyl group R′ on Hg (cf. **2** vs **7**) precludes a Hg(II)-centered origin for these transitions. However, the absorption features show bathochromic shifts when the Hg(II) fragments are introduced at the terminal groups, and such a red-shift reveals π-delocalization through the Hg centers due to metal to ligand back-donation to π*(C≡CR). On the basis of the observed data, the spectra are probably dominated by ligand-based π−π* transitions, but mixed with a small contribution from the metal in the HOMO and the LUMO. This agrees well with the molecular orbital calculations on **1** and **2**. Figure 7 depicts the contour plots of the HOMO and LUMO for **1** and **2**, showing the common bonding feature in the frontier molecular orbitals. The calculated HOMO−LUMO gap follows the order **1** (4.19 eV) > **2** (3.76 eV), in line with our experimental observations. The metal contributions based on the Mulliken population analysis[17] to the HOMO and LUMO are small in

(15) Li, P.; Ahrens, B.; Choi, K.-H.; Khan, M. S.; Raithby, P. R.; Wilson, P. J.; Wong, W.-Y. *CrystEngComm*. **2002**, *4*, 405.

(16) (a) Gutierrez-Puebla, E.; Vegas, A.; Garcia-Blanco, S. *Cryst. Struct. Commun*. **1979**, *8*, 861. (b) Gutierrez-Puebla, E.; Vegas A.; Garcia-Blanco, S. *Acta Crystallogr. Sect. B* **1978**, *34*, 3382. (c) Hoskins, B. F.; Robson R.; Sutherland, E. E. *J. Organomet. Chem*. **1996**, *515*, 259. (d) Hartbaum, C.; Roth, G.; Fischer, H. *Eur. J. Inorg. Chem*. **1998**, 191. (e) Ghosh, I.; Mishra, R.; Poddar, D.; Mukherjee, A. K. *Chem. Commun*. **1996**, 435.

(17) *MullPop*, a program written by Reinaldo Pis Diez at the National University of La Plata, Argentina.

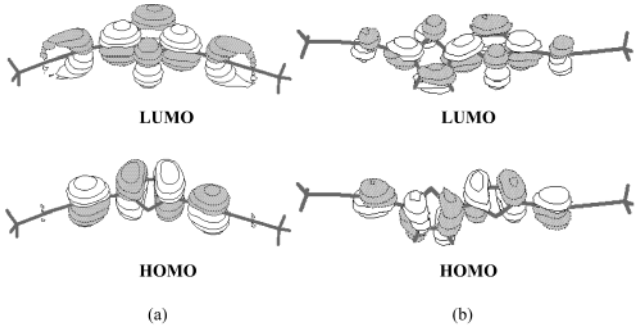

Figure 7. Spatial plots of the highest occupied (HOMO) and lowest unoccupied (LUMO) molecular orbitals for (a) **1** and (b) **2**.

both cases (HOMO 3.0%, LUMO 20.0% from each Hg for **1**; HOMO 1.5%, LUMO 7.0% from each Hg for **2**).

The effect of attachment of the mercury(II) moiety is found to lower the transition energies and to increase the absorption intensity, indicating an enhancement in the degree of π-delocalization through the mercury conjugated system, but the extent of the red-shift is smaller as compared to that imparted by the $[AuPPh_3]^+$ moiety (e.g., 293 **Ib**, 337 **1**, 361 nm $[Ph_3PAuC{\equiv}C\text{-}(C_4H_2S)C{\equiv}CAuPPh_3]$).[15] The more marked effect for Au(I) is consistent with the lower oxidation state of +1 in gold(I) complexes, which would enhance the back-donation to π^*. Increasing conjugation through more thienyl rings leads to a decreased transition energy and an increase in the molar absorption coefficients for **1**−**3** as well as **6**−**8**. Thus, a red-shift of ca. 75 nm is observed from **1** to **3**, whereas the shift is 71 nm from **6** to **8**. However, the value of the red-shift induced by the end substitution of Hg(II) groups decreases with increasing number of thienyl units.[9c,18] These results are also consistent with the mercury-based orbitals contributing less to the HOMO and LUMO levels as the number of thiophene rings increases (vide supra) and hence π-conjugation increases. It is noteworthy that replacing the bithiophene spacer as in **2** by a bithiazole moiety in **4** and **5** notably lowers the HOMO−LUMO gap, suggestive of enhanced conjugation in the latter. The bathochromic shift of 10−20 nm compared to their bithienyl counterparts can be ascribed to the presence of the electron-withdrawing imine nitrogen atoms in the bithiazole derivatives.[11,12] The absorption peak of **5** (or **10**) is also red-shifted relative to **4** (or **9**), presumably due to the more extensive conjugation via the π-phenylene unit along with the π-donating capacity of the OMe group in the former case.

Complexes **1**−**10** are all emissive at room temperature, and the emission maxima roughly follow the same order as the absorption energies. These featureless luminescence spectra are independent of the excitation wavelength used. The emission energy was found to change upon variation of the central organic linkers R (Figure 8) but does not vary much with respect to the nature of R′. Their similar spectral patterns as their free alkynes are suggestive of the ligand-dominating emissive state, and thus the lowest emissive states in these complexes can tentatively be assigned as metal-perturbed $\pi-\pi^*$ transitions. The orders of emission energies **1** > **2** > **3** and **6** > **7** > **8** are expected in moving from the monothiophene to the terthiophene. On the other hand, we observe a notable but not dramatic quenching effect on going from the purely organic precursors to the Hg-bound species as far as emission quantum yields are concerned. With reference to previous work on other mercury acetylide systems or alike,[8] we can possibly attribute the quenching in the luminescence intensity to the so-called heavy-atom effect, which catalyzes the nonradiative deactivation of the excited states of the fluorophore. Due to the lack of available low-lying metal-localized excited states, it is unlikely that energy or electron-transfer quenching mechanism operates here.[8,19] It is also clear that there is an increase in quantum yield with increasing *n* value, and the values associated with 4,4′-di(*tert*-butyl)-2,2′-bithiazole-linked complexes are higher than those for the bithienyl congeners.

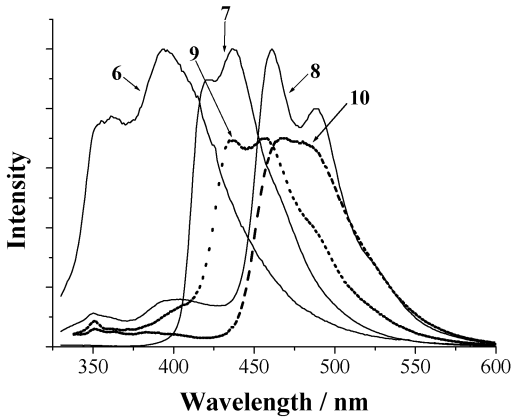

Figure 8. Emission spectra of **6**−**10** in CH_2Cl_2 solutions at 298 K.

Concluding Remarks

The present work reports a high-yield synthetic access to a new series of luminescent binuclear mercury(II) bis(alkynyl) complexes bearing oligothiophene and bithiazole conjugated units. Electronic absorption and photophysical properties of these compounds have been studied in terms of the oligothienyl chain length and the electronic nature of the five-membered heterocycle, and the data were compared with those in their isolobal gold(I) counterparts. The formation of polymeric mercury acetylide systems in the solid state through Hg···Hg and Hg···S interactions is observed. Moreover, the results here demonstrate that absorption and emission maxima can be increased either by increasing the chain length or by incorporation of a thiazole unit consisting of electron-donating heterocyclic units (p-doping) and electron-withdrawing imine groups (n-doping). Addition of Hg(II) units decreases the energy of the $\pi-\pi^*$ transition in the heteroaromatic bridge, which is consistent with the theoretical calculations, and increases the absorption intensity. The quenching effect observed should provide valuable information to our understanding of the development of new molecular luminescent sensing systems for organomercurials.

(18) Garcia, P.; Pernaut, J. M.; Hapiot, P.; Wintgens, V.; Valat, P.; Garnier, F.; Delabouglise, D. *J. Phys. Chem.* **1993**, *97*, 513.

(19) Prodi, L.; Bolletta, F.; Montalti, M.; Zaccheroni, N. *Eur. J. Inorg. Chem.* **1999**, 455.

Experimental Section

General Comments. All reactions were conducted under an atmosphere of dry nitrogen with the use of standard Schlenk techniques. Solvents for preparative work were dried and distilled before use. IR spectra were obtained using a Nicolet FTIR-550 spectrometer. NMR spectra were recorded in $CDCl_3$ on a JEOL JNM-EX 270 or a Varian Inova 400 MHz FT-NMR spectrometer. Electron impact (EI) and fast atom bombardment (FAB) mass spectra were recorded on a Finnigan-SSQ 710 spectrometer. Electronic absorption and luminescence spectra were measured in appropriate solvents with a Varian Cary 100 UV/vis spectrophotometer and a PTI luminescence spectrometer, respectively. The luminescence quantum yields were determined in CH_2Cl_2 solutions at 290 K against the anthracene standard in the same solvent (Φ = 0.27).[20] Unless otherwise stated, all reagents were from commercial sources and used as received. The starting precursors 2,5-diethynylthiophene (**Ib**), 5,5′-diethynyl-2,2′-bithiophene (**IIb**), and 5,5″-diethynyl-2,2′:5′,2″-terthiophene **(IIIb)** were prepared according to the reported procedures.[9a] Purification of diethynyl ligands was accomplished by column chromatography on silica or preparative silica TLC plates (Merck, Kieselgel 60). Density functional calculations at the B3LYP level[21] were performed on **1** and **2** on the basis of their experimentally determined geometries obtained from crystallographic data. The basis set used for C, O, and H atoms was 6-31G,[22] while effective core potentials with a LanL2DZ basis set[23] were employed for S and Hg atoms. The Gaussian 98 program was used for the calculations.[24] Polarization functions were added for S atoms (ξ_d(S) = 0.421). **CAUTION:** Organomercurials are toxic, and all experimentation involving these reagents should be carried out in a well-vented hood.

MeHgC≡CRC≡CHgMe (R = thiophene-2,5-diyl) 1. MeHgCl (45.2 mg, 0.18 mmol) in MeOH (15 mL) was mixed with freshly prepared 2,5-diethynylthiophene (**Ib**, 11.9 mg, 0.09 mmol) in CH_2Cl_2 (5 mL). To this solution mixture was added 4 mL of basic MeOH (0.80 mmol, prepared by dissolving 0.20 g of NaOH in 25 mL of MeOH). Within a few minutes, a pale yellow solid precipitated from the homogeneous solution. The solid was collected after stirring for 2 h, washed with MeOH, and air-dried to provide **1** in 82% yield (41.4 mg). IR (CH_2Cl_2): ν(C≡C) 2118 cm^{-1}. ^{1}H NMR ($CDCl_3$): δ 0.57 (s, $^2J_{HgH}$ = 148 Hz, 6H, Me), 6.98 (s, 2H, thienyl). FAB-MS (*m*/*z*): 561 [M$^+$]. Anal. Calcd for $C_{10}H_8Hg_2S$: C, 21.28; H, 1.43. Found: C, 21.03; H, 1.35.

MeHgC≡CRC≡CHgMe (R = [2,2′]bithiophene-5,5′-diyl) 2. Compound **2** was prepared using the same conditions described above for **1**, but 5,5′-diethynyl-2,2′-bithiophene (**IIb**, 19.3 mg, 0.09 mmol) was used instead to afford a yellow solid in 88% yield (51.0 mg). IR (CH_2Cl_2): ν(C≡C) 2123 cm^{-1}. ^{1}H NMR ($CDCl_3$): δ 0.72 (s, $^2J_{HgH}$ = 148 Hz, 6H, Me), 6.98 (d, J_{HH} = 3.8 Hz, 2H, thienyl), 7.07 (d, J_{HH} = 3.8 Hz, 2H, thienyl). FABMS (*m*/*z*): 643 [M$^+$]. Anal. Calcd for $C_{14}H_{10}Hg_2S_2$: C, 26.13; H, 1.57. Found: C, 26.05; H, 1.55.

MeHgC≡CRC≡CHgMe (R = [2,2′:5′2″]terthiophene-5,5″-diyl) 3. Complex **3** was similarly synthesized from 5,5″-diethynyl-2,2′:5′,2″-terthiophene (**IIIb**, 26.6 mg, 0.09 mmol), and it was isolated as an orange powder in 74% yield (48.4 mg). IR (CH_2Cl_2): ν(C≡C) 2123 cm^{-1}. ^{1}H NMR ($CDCl_3$): δ 0.72 (s, $^2J_{HgH}$ = 148 Hz, 6H, Me), 7.00 (d, J_{HH} = 3.8 Hz, 2H, thienyl), 7.05 (s, 2H, thienyl), 7.09 (d, J_{HH} = 3.8 Hz, 2H, thienyl). FABMS (*m*/*z*): 726 [M$^+$]. Anal. Calcd for $C_{18}H_{12}Hg_2S_3$: C, 29.79; H, 1.67. Found: C, 29.50; H, 1.57.

MeHgC≡CRC≡CHgMe (R = 4,4′-di(*tert*-butyl)-2,2′-bithiazole-5,5′-diyl) 4. A procedure similar to that illustrated for **1** was used to obtain the title compound in 90% yield (61.4 mg) from 5,5′-diethynyl-4,4′-di(*tert*-butyl)-2,2′-bithiazole (**IVb**, 29.5 mg, 0.09 mmol). IR (CH_2Cl_2): ν(C≡C) 2125 cm^{-1}. ^{1}H NMR ($CDCl_3$): δ 0.73 (s, $^2J_{HgH}$ = 151 Hz, 6H, Me), 1.46 (s, 18H, CMe_3). FABMS (*m*/*z*): 758 [M$^+$]. Anal. Calcd for $C_{20}H_{24}N_2Hg_2S_2$: C, 31.70; H, 3.19; N, 3.70. Found: C, 31.47; H, 3.04; N, 3.58.

MeHgC≡CRC≡CHgMe (R = 4,4′-di(*p*-methoxyphenylene)-2,2′-bithiazole-5,5′-diyl) 5. Additon of an excess of basic MeOH to a mixture of MeHgCl (25.1 mg, 0.10 mmol) in MeOH and 5,5′-diethynyl-4,4′-di(*p*-methoxyphenylene)-2,2′-bithiazole (**Vb**, 21.4 mg, 0.05 mmol) in CH_2Cl_2 leads to the precipitation of **5** as an orange solid in 87% yield (37.3 mg). IR (CH_2Cl_2): ν(C≡C) 2123 cm^{-1}. ^{1}H NMR ($CDCl_3$): δ 0.76 (s, $^2J_{HgH}$ = 150 Hz, 6H, Me), 3.87 (s, 6H, OMe), 7.00 (d, J_{HH} = 8.4 Hz, 4H, C_6H_4), 8.31 (d, J_{HH} = 8.4 Hz, 4H, C_6H_4). FABMS (*m*/*z*): 858 [M$^+$]. Anal. Calcd for $C_{26}H_{20}N_2Hg_2O_2S_2$: C, 36.41; H, 2.35; N, 3.27. Found: C, 36.21; H, 2.24; N, 3.19.

PhHgC≡CRC≡CHgPh (R = thiophene-2,5-diyl) 6. The freshly prepared diyne **Ib** (11.9 mg, 0.09 mmol) in CH_2Cl_2 (5 mL) was first combined with PhHgCl (56.4 mg, 0.18 mmol) in MeOH (15 mL), and 0.2 M basic MeOH (4 mL) was subsequently added to give a pale yellow suspension. The solvents were then decanted, and the light-yellow powder of **6** (50.6 mg, 82%) was air-dried. IR (KBr): ν(C≡C) 2115 cm^{-1}. ^{1}H NMR ($CDCl_3$): δ 7.08 (s, 2H, thienyl), 7.31−7.38 (m, 10H, Ph). FABMS (*m*/*z*): 685 [M$^+$]. Anal. Calcd for $C_{20}H_{12}Hg_2S$: C, 35.04; H, 1.76. Found: C, 35.01; H, 1.67.

PhHgC≡CRC≡CHgPh (R = [2,2′]bithiophene-5,5′-diyl) 7. Instead of using MeHgCl, the dehydrohalogenation reaction between PhHgCl (25.1 mg, 0.08 mmol) and **IIb** (8.6 mg, 0.04 mmol) in basic MeOH solution resulted in the precipitation of the title product **7** as a yellow solid (23.8 mg, 88%). IR (CH_2Cl_2): ν(C≡C) 2126 cm^{-1}. ^{1}H NMR ($CDCl_3$): δ 7.03 (d, J_{HH} = 3.8 Hz, 2H, thienyl), 7.14 (d, J_{HH} = 3.8 Hz, 2H, thienyl), 7.32 (m, 6H, Ph), 7.40 (m, 4H, Ph). FABMS (*m*/*z*): 768 [M$^+$]. Anal. Calcd for $C_{24}H_{14}Hg_2S_2$: C, 37.55; H, 1.84. Found: C, 37.26; H, 1.64.

PhHgC≡CRC≡CHgPh (R = [2,2′:5′2″]terthiophene-5,5″-diyl) 8. Similar to **6**, complex **8** was prepared from **IIIb** (26.6 mg, 0.09 mmol) and collected as an orange solid with a yield of 74% (56.6 mg) after filtration and washing. IR (CH_2Cl_2): ν(C≡C) 2127 cm^{-1}. ^{1}H NMR ($CDCl_3$): δ 7.03 (d, J_{HH} = 3.8 Hz, 2H, thienyl), 7.08 (s, 2H, thienyl), 7.15 (d, J_{HH} = 3.8 Hz, 2H, thienyl), 7.32 (m, 6H, Ph), 7.41 (m, 4H, Ph). FABMS (*m*/*z*): 850 [M$^+$]. Anal. Calcd for $C_{28}H_{16}Hg_2S_3$: C, 39.58; H, 1.90. Found: C, 39.29; H, 1.80.

PhHgC≡CRC≡CHgPh (R = 4,4′-di(*tert*-butyl)-2,2′-bithiazole-5,5′-diyl) 9. A procedure similar to that used for **6** was used to obtain the title compound in 70% yield (55.6 mg) from **IVb** (29.5 mg, 0.09 mmol). IR (CH_2Cl_2): ν(C≡C) 2128 cm^{-1}. ^{1}H NMR ($CDCl_3$): δ 1.56 (s, 18H, CMe_3), 7.35 (m, 6H, Ph), 7.42 (m, 4H, Ph). FABMS (*m*/*z*): 882 [M$^+$]. Anal. Calcd for $C_{30}H_{28}N_2Hg_2S_2$: C, 40.86; H, 3.20; N, 3.18. Found: C, 40.56; H, 3.10; N, 3.05.

PhHgC≡CRC≡CHgPh (R = 4,4′-di(*p*-methoxyphenylene)-2,2′-bithiazole-5,5′-diyl) 10. A procedure similar to that for **6** was employed using **Vb** (38.5 mg, 0.09 mmol) to provide orange **10** in 74% yield (65.4 mg). IR (CH_2Cl_2): ν(C≡C) 2120 cm^{-1}. ^{1}H NMR ($CDCl_3$): δ 7.01 (d, J_{HH} = 8.4 Hz, 4H,

(20) Dawson, W. R.; Windsor, M. W. *J. Phys. Chem.* **1968**, *72*, 3251.
(21) (a) Decke, A. D. *J. Chem. Phys.* **1993**, *98*, 5648. (b) Miehlich, B.; Savin, A.; Stoll, H.; Preuss, H. *Chem. Phys. Lett.* **1989**, *157*, 200. (c) Lee, C.; Yang, W.; Parr, G. *Phys. Rev. B* **1988**, *37*, 785.
(22) Hariharan, P. C.; Pople, J. A. *Theor. Chim. Acta* **1973**, *28*, 213.
(23) Hay, P. J.; Wadt, W. R. *J. Chem. Phys.* **1985**, *82*, 299.
(24) Frisch, M. J.; Trucks, G. W.; Schlegel, H. B.; Scuseria, G. E.; Robb, M. A.; Cheeseman, J. R.; Zakrzewski, V. G.; Montgomery, J. A., Jr.; Stratmann, R. E.; Burant, J. C.; Dapprich, S.; Millam, J. M.; Daniels, A. D.; Kudin, K. N.; Strain, M. C.; Farkas, O.; Tomasi, J.; Barone, V.; Cossi, M.; Cammi, R.; Mennucci, B.; Pomelli, C.; Adamo, C.; Clifford, S.; Ochterski, J.; Petersson, G. A.; Ayala, P. Y.; Cui, Q.; Morokuma, K.; Malick, D. K.; Rabuck, A. D.; Raghavachari, K.; Foresman, J. B.; Cioslowski, J.; Ortiz, J. V.; Stefanov, B. B.; Liu, G.; Liashenko, A.; Piskorz, P.; Komaromi, I.; Gomperts, R.; Martin, R. L.; Fox, D. J.; Keith, T.; Al-Laham, M. A.; Peng, C. Y.; Nanayakkara, A.; Gonzalez, C.; Challacombe, M.; Gill, P. M. W.; Johnson, B.; Chen, W.; Wong, M. W.; Andres, J. L.; Gonzalez, C.; Head-Gordon, M.; Replogle, E. S.; Pople, J. A. *Gaussian 98* (Revision A.5); Gaussian, Inc.: Pittsburgh, PA, 1998.

Table 4. Summary of Crystal Structure Data for Compounds IVa, Va, 1, and 2

	IVa	Va	1	2
empirical formula	$C_{24}H_{36}N_2S_2Si_2$	$C_{30}H_{32}N_2O_2S_2Si_2$	$C_{10}H_8Hg_2S$	$C_{14}H_{10}Hg_2S_2$
fw	472.85	572.88	561.40	643.52
cryst size, mm	0.30 × 0.14 ×0.13	0.39 × 0.08 × 0.06	0.23 × 0.16 × 0.12	0.26 × 0.10 × 0.08
cryst syst	monoclinic	triclinic	monoclinic	triclinic
space group	$P2_1/n$	$P\bar{1}$	$P2_1/c$	$P\bar{1}$
a, Å	5.9333(8)	5.7604(6)	9.710(2)	8.5731(16)
b, Å	20.621(3)	11.6894(12)	14.469(3)	8.9250(17)
c, Å	11.8559(16)	11.9504(13)	8.610(2)	9.8628(18)
α, deg	90	97.465(2)	90	89.031(4)
β, deg	94.301(2)	100.537(2)	111.041(4)	88.823(4)
γ, deg	90	97.548(2)	90	73.136(3)
V, Å^3	1446.5(3)	774.42(14)	1129.0(5)	722.0(2)
Z	2	1	4	2
D_{calcd}, g cm^{-3}	1.086	1.228	3.303	2.960
μ, mm^{-1}	0.280	0.278	27.300	21.505
F(000)	508	302	976	572
temp, K	293	293	293	293
θ range, deg	1.98−24.99	1.76−25.00	2.25−25.00	2.07−25.00
no. of reflns collected	7127	3890	5538	3562
no. of unique reflns (*R*(int))	2529 (0.0216)	2670 (0.0209)	1988 (0.0714)	2469 (0.0305)
no. of reflns with $I > 2\sigma(I)$	2529	2670	1988	2469
no. of params	142	203	119	164
R1, wR2 [$I > 2\sigma(I)$][a]	0.0466, 0.1590	0.0528, 0.1445	0.0494, 0.1395	0.0624, 0.1641
R1, wR2 (all data)[a]	0.0568, 0.1794	0.0686, 0.1595	0.0551, 0.1462	0.0719, 0.1706
goodness of fit	0.854	1.014	0.992	0.960
largest diff peak and hole, e Å^{-3}	0.504 and −0.261	0.355 and −0.248	2.228 and −2.433	2.634 and −1.824

[a] $R1 = \sum||F_o| - |F_c||/\sum|F_o|$, $wR2 = [\sum w(|F_o^2| - |F_c^2|)^2/\sum w|F_o^2|^2]^{1/2}$.

C_6H_4), 7.39 (m, 6H, Ph), 8.15 (m, 4H, Ph), 8.34 (d, $J_{HH} = 8.4$ Hz, 4H, C_6H_4). FABMS (*m*/*z*): 982 [M$^+$]. Anal. Calcd for $C_{36}H_{24}N_2Hg_2O_2S_2$: C, 44.04; H, 2.46; N, 2.85. Found: C, 43.89; H, 2.26; N, 2.53.

Crystallography. Yellow crystals of **IVa**, **Va**, **1**, and **2** suitable for X-ray diffraction analyses were grown by evaporation of their respective solutions in a hexane−CH_2Cl_2 mixture. Geometric and intensity data were collected using graphite-monochromated Mo Kα radiation ($\lambda = 0.71073$ Å) on a Bruker AXS SMART CCD area-detector. The diffraction frames were integrated using the SAINT package[25] and corrected for absorption with SADABS.[26] The structure was solved by the Patterson (for **1**) and direct methods (for **IVb**, **Vb**, and **2**) (SHELXTL[27]) in conjunction with standard difference Fourier techniques and subsequently refined by full-matrix least-squares analyses. All non-hydrogen atoms were refined anisotropically. Hydrogen atoms were generated in their idealized positions and allowed to ride on the respective carbon atoms. The largest electron residuals are all close to the heavy Hg atoms. Crystallographic and other experimental details are collected in Table 4.

Acknowledgment. We thank the Hong Kong Research Grants Council (Grant No. HKBU 2048/01P) and the Hong Kong Baptist University (Grant No. FRG/99-00/II-58) for financial support.

Supporting Information Available: Preparations of bithiazole-based precursors and tables of X-ray crystal data for the new compounds. This material is available free of charge via the Internet at http://pubs.acs.org.

OM020517E

(25) *SAINT Reference Manual*; Siemens Energy and Automation: Madison, WI, 1994−1996.
(26) Sheldrick, G. M. *SADABS*, Empirical Absorption Correction Program; University of Göttingen: Germany, 1997.
(27) Sheldrick, G. M. *SHELXTL Reference Manual*, version 5.1; Siemens Energy and Automation: Madison, WI, 1997.